https://doi.org/10.5194/egusphere-2023-2370
Preprint. Discussion started: 16 November 2023

Evaluation of CMIP6 model simulations of $PM_{2.5}$ and its components over China

Fangxuan Ren[1], Jintai Lin[1], Chenghao Xu[1], Jamiu A. Adeniran[1], Jingxu Wang[2], Randall V. Martin[3], Aaron van Donkelaar[3], Melanie S. Hammer[4], Larry W. Horowitz[5], Steven T. Turnock[6, 7], Naga Oshima[8], Jie Zhang[9], Susanne Bauer[10], Kostas Tsigaridis[11, 10], Øyvind Seland[12], Pierre Nabat[13], David Neubauer[14], Gary Strand[15], Twan van Noije[16], Philippe Le Sager[16], Toshihiko Takemura[17]

[1] Laboratory for Climate and Ocean-Atmosphere Studies, Department of Atmospheric and Oceanic Sciences, School of Physics, Peking University, Beijing 100871, China
[2] Frontier Science Center for Deep Ocean Multispheres and Earth System (FDOMES) and Physical Oceanography Laboratory, College of Oceanic and Atmospheric Sciences, Ocean University of China, Qingdao 266100, China
[3] Department of Energy, Environmental, and Chemical Engineering, Washington University, St. Louis, MO, USA
[4] St. Francis Xavier University, Department of Earth Sciences, Antigonish, NS, Canada
[5] NOAA Geophysical Fluid Dynamics Laboratory, Princeton, NJ, USA
[6] Met Office Hadley Center, Exeter, UK
[7] University of Leeds Met Office Strategic (LUMOS) Research Group, University of Leeds, UK
[8] Meteorological Research Institute, Tsukuba, Japan
[9] Beijing Climate Center, China Meteorological Administration, Beijing 100081, China
[10] NASA Goddard Institute for Space Studies, New York, NY, USA
[11] Center for Climate Systems Research, Columbia University, New York, NY, USA
[12] Norwegian Meteorological Institute, P.O. Box 43 Blindern, Oslo, Norway
[13] Centre National de Recherches Météorologiques (CNRM), Météo-France, CNRS, Toulouse, France
[14] Institute of Atmospheric and Climate Science, ETH Zurich, Zurich, Switzerland
[15] Climate and Global Dynamics Laboratory, the National Center for Atmospheric Research, Boulder, CO, USA
[16] Royal Netherlands Meteorological Institute, De Bilt, Netherlands
[17] Research Institute for Applied Mechanics, Kyushu University, Fukuoka, Japan

Correspondence to: Jintai Lin (linjt@pku.edu.cn)

Abstract. Earth system models (ESMs) participating in the latest Coupled Model Intercomparison Project Phase 6 (CMIP6) simulate various components of fine particulate matter ($PM_{2.5}$) as major climate forcers. Yet the model performance for $PM_{2.5}$ components remains little evaluated due in part to lack of observational data. Here, we evaluate near-surface concentrations of $PM_{2.5}$ and its five main components over China as simulated by fourteen CMIP6 models, including organic carbon (OC, available in 14 models), black carbon (BC, 14 models), sulfate (14 models), nitrate (4 models), and ammonium (5 models). For this purpose, we collect observational data between 2000 and 2014 from a satellite-based

https://doi.org/10.5194/egusphere-2023-2370
Preprint. Discussion started: 16 November 2023

dataset for total $PM_{2.5}$ and from 2469 measurement records in the literature for $PM_{2.5}$ components. Seven models output total $PM_{2.5}$ concentrations, and they all underestimate the observed total $PM_{2.5}$ over eastern China, with GFDL-ESM4 (–1.5%) and MPI-ESM-1-2-HAM (–1.1%) exhibiting the smallest biases averaged over the whole country. The other seven models, for which we recalculate total $PM_{2.5}$ from the available components output, underestimate the total $PM_{2.5}$ concentrations, partly because of the missing model representations of nitrate and ammonium. Concentrations of the five individual components are underestimated in almost all models, except that sulfate is overestimated in MPI-ESM-1-2-HAM by 12.6% and in MRI-ESM2-0 by 24.5%. The underestimation is the largest for OC (by –71.2% to –37.8% across the 14 models) and the smallest for BC (–47.9% to –12.1%). The multi-model mean (MMM) reproduces fairly well the observed spatial pattern for OC (R = 0.51), sulfate (R = 0.57), nitrate (R = 0.70) and ammonium (R = 0.75), yet the agreement is poorer for BC (R = 0.39). The varying performances of ESMs on total $PM_{2.5}$ and its components have important implications for the modeled magnitude and spatial pattern of aerosol radiative forcing.

1 Introduction

Fine particulate matter ($PM_{2.5}$) influences air quality, human health and climate change. Exposure to near-surface $PM_{2.5}$ is associated with millions of global premature deaths each year (Zhang et al., 2017; World Health Organization, 2021). $PM_{2.5}$ affects the radiative budget of the climate system directly through scattering and absorption and indirectly via clouds. The effects of atmospheric aerosols on cloud droplet concentrations, cloud distributions and radiative properties pose large uncertainties in the estimating radiative forcing (Carslaw et al., 2013; Seinfeld et al., 2016). Earth system models (ESMs) are essential tools for studying global climate change. The accuracy of $PM_{2.5}$ simulations in ESMs exhibits a crucial constraint on the reliability of these models in climate change simulation and projection. The Coupled Model Intercomparison Project Phase 6 (CMIP6) provides an opportunity to evaluate simulated $PM_{2.5}$ and its components by the current-generation ESMs, which implement interactive aerosol and atmospheric chemistry (Turnock et al., 2020). A total of 21 ESMs participating in CMIP6 provide total $PM_{2.5}$ and/or several component simulations, although the aerosol component species vary across these models. Fourteen models include organic aerosol (OA, converted to organic carbon (OC) in this study by assuming OA / OC = 1.6), black carbon (BC), sulfate, dust (DST), and sea salt (SSLT). Four of these

https://doi.org/10.5194/egusphere-2023-2370
Preprint. Discussion started: 16 November 2023

14 models also include nitrate and five include ammonium (Table S1).

Aerosol optical depth (AOD) during 2000–2014 simulated in CMIP5 and CMIP6 are in broad agreement with satellite retrievals over most parts of Europe, North America, and India (Zhang et al., 2022; Cherian and Quaas, 2020). CMIP6 models better capture satellite-based AOD trends in western North America and eastern China, whereas CMIP5 models failed to reproduce the trends in AOD (Mortier et al., 2020; Cherian and Quaas, 2020). Studies have emerged over recent years to assess the CMIP model performance of individual aerosol components. An assessment of CMIP5 dust aerosol simulations using independent data from 1851 to 2011 over North Africa shows a common underestimate (Evan et al., 2016). Another analysis of CMIP3 and CMIP5 models suggests sea salt aerosols over the tropical Pacific to be significantly underestimated (Chen et al., 2020). Evaluation of the vertical distribution of BC in CMIP5 models based on aircraft measurements shows an overestimate in the upper troposphere especially over the Central Pacific (Allen and Landuyt, 2014). Several CMIP5 models produce high sulfate burdens over eastern China, the Indian Peninsula and the northern Indo-Chinese Peninsula, although the transport difference among these models results in distinctive spatial distributions (Li et al., 2020). Overall, global climate models struggle to accurately reproduce observed aerosol component concentrations over different world regions.

China is a major region with heavy aerosol pollution, dense population and complex climate, and thus it is critical to understand the performance of ESMs for aerosol simulations over this country. Several studies have evaluated total $PM_{2.5}$ simulations of CMIP models over China, using AOD data from satellite retrievals and ground-based aerosol networks (Mortier et al., 2020; Sockol and Small Griswold, 2017; Michou et al., 2020). They find that CMIP5 models reproduce the spatial pattern of AOD reasonably well over eastern China, but with a tendency to underestimate AOD magnitudes (Liu and Liao, 2017; Park et al., 2014; Allen et al., 2013). GFDL-CM3 performs best among CMIP5 models in simulating AOD over eastern China, partly because it includes nitrate and ammonium that most models lack (Li et al., 2020). Other studies suggest that CMIP6 models simulate the magnitude of annual mean AOD better than CMIP5 over eastern China, in part due to the notable increase in sulfate (Cherian and Quaas, 2020; Fan et al., 2018a). Nonetheless, the CMIP6 models fail to capture the seasonal north-south shift of AOD maximum center (Li et al., 2021; Wang et al., 2021).

https://doi.org/10.5194/egusphere-2023-2370
Preprint. Discussion started: 16 November 2023

Different $PM_{2.5}$ components exhibit distinctive radiative effects, thus understanding the performance of ESMs in simulating individual $PM_{2.5}$ components is important. Due to the absence of publicly available observational component data over China, only a few studies target single aerosol components (such as sulfate and dust) over a large region of the country, or different $PM_{2.5}$ components over a short period or a small region (Pu and Ginoux, 2018; Zhao et al., 2022). For example, model evaluation based on the Acid Deposition Monitoring Network in East Asia (EANET) suggests that sulfate concentrations simulated by CMIP5 and CMIP6 show a rising trend similar to observations (Mulcahy et al., 2020), but the simulations are still lower than observed concentrations (Fan et al., 2018b; Mortier et al., 2020). A recent study compares $PM_{2.5}$ components (dust, sea salt, BC, OC and sulfate) in CMIP6 models with the Modern Era Retrospective analysis for Research and Applications Aerosol Reanalysis (MERRAero) in Asia from 2005 to 2020 (Su et al., 2022; Buchard et al., 2016). The study shows that CMIP6 model uncertainties of total $PM_{2.5}$ over East Asia are mainly attributable to sulfate and mineral dust simulations. However, the model biases may in part come from other components (nitrate and ammonium) that are not analyzed in their study; and the MERRAero data might contain errors as well (Ma et al., 2021; Mahesh et al., 2019).

In this study, we evaluate near-surface concentrations of $PM_{2.5}$ and its five main components (OC, BC, sulfate, nitrate, and ammonium) from 2000 to 2014 over China simulated by fourteen CMIP6 models driven by historical emissions. For this purpose, we employ a satellite-based dataset for total $PM_{2.5}$ concentrations and a self-compiled $PM_{2.5}$ component dataset from 221 ground stations during 2000–2014 collected from the literature. Section 2 introduces CMIP6 model simulations, satellite-based total $PM_{2.5}$ concentration data, and literature-based $PM_{2.5}$ component data. Section 3 assesses the performance of CMIP6 models for total $PM_{2.5}$. Section 4 evaluates the simulated $PM_{2.5}$ components. Section 5 discusses the climate implications of the inadequacies in total $PM_{2.5}$ and its components in CMIP6 models. Section 6 concludes the study.

2 Data and method

2.1 CMIP6 simulations

Near-surface concentrations of total $PM_{2.5}$ and its components can be converted from dry aerosol mass mixing ratios (MMRs) in CMIP6 models. Monthly mean near-surface MMRs (in the lowest model layer)

https://doi.org/10.5194/egusphere-2023-2370
Preprint. Discussion started: 16 November 2023

of $PM_{2.5}$ and its main components are taken from fourteen CMIP6 models to assess the performance of ESMs over China (Table S1). Data are obtained from the "Historical" experiments covering 1850−2014, which serve as the entry cards for participating in CMIP6 (Eyring et al., 2016). They are coupled atmosphere-ocean simulations that include all CMIP6 historical forcings, and are well suited for quantifying and understanding model characteristics. The ensemble mean is taken for each model by averaging all available ensemble members. For GISS models, the ensemble members use two physics configurations with drastically different aerosol parameterizations. We average the ensemble members using the same physics configurations in GISS models, named GISS-E2-1-OMA (physics-version = 3) and GISS-E2-1-MATRIX (physics-version = 5) respectively (Bauer et al., 2020). Simulation results over 2000−2014 are selected and re-gridded to 1° × 1° for comparison with available satellite- and ground-based data.

The anthropogenic emission data (ver. 2016-07-26) to drive "Historical" CMIP6 simulations is produced by the Community Emissions Data System (CEDS) (Hoesly et al., 2018). An updated version of CEDS (ver. 2017-05-18) corrected several errors in the spatial distribution within each country, but does not change total emissions by country and sector (Feng et al., 2020). The CEDS emissions (ver. 2016-07-26 and ver. 2017-05-18) of OC, BC, CO, NO_x and SO_2 in China after 2000 are higher than those in the MEIC (Paulot et al., 2018; Zheng et al., 2018) inventory and the Peking University (PKU) inventory (Wang et al., 2014; Huang et al., 2015; Tao et al., 2018) which use more detailed Chinese data. This difference in China has been reduced when CEDS was used to derive future SSP scenarios in CMIP6 simulations (published on ESGF on 28 June 2018 on https://esgf-node.llnl.gov/search/cmip6), and has been included in a post-CMIP6 version of CEDS (McDuffie et al., 2020).

Of the fourteen models, all output the MMRs of OA, BC, sulfate, dust and sea salt, five output ammonium, and four output nitrate (Table S1). Seven models output the MMRs of total $PM_{2.5}$, as the sum over all components with suitable particle sizes. The MMRs are converted to mass concentrations ($\mu g\ m^{-3}$) based on air density in each model. In evaluating $PM_{2.5}$ components (Sect. 2.3), modeled OA is converted to organic carbon (OC) to be comparable with the observational dataset. Modeled OA refers to total organic aerosol, including primary organic aerosol (POA) and secondary organic aerosol (SOA). For the GFDL-ESM4 model, the "mmroa" variable for OA only includes POA; thus we calculate the total OA of GFDL-

https://doi.org/10.5194/egusphere-2023-2370
Preprint. Discussion started: 16 November 2023

ESM4 as mmroa plus mmrsoa. The OA/OC ratios in the literature range from 1.4 to 2.1 (Bürki et al., 2020; Lin et al., 2016). We choose an OA/OC ratio of 1.6, which is the same as the ratio used in converting near-surface OA observations to OC. This ratio is slightly higher than the value of 1.4 recommended by CMIP6 for POA, but it does not affect the relative (percentage) model bias found in this study because the same ratio is used for models and observations.

For the seven models that do not output total $PM_{2.5}$, we follow the previous work to estimate total $PM_{2.5}$ concentrations (Eq. 1) (Turnock et al., 2020). Here, OA, BC, sulfate and certain portions of sea salt (SSLT, a_1) and dust (DST, a_2) are assumed to be present in fine particles (diameter < 2.5 μm).

$$PM_{2.5} = OA + BC + SO_4^{2-} + a_1 \times SSLT + a_2 \times DST \quad (1)$$

For most models, specific values of a_1 and a_2 are provided by model developers (Table S2). BCC-ESM1 does not provide the coefficients. Instead, the model outputs concentrations in four size bins for each of dust (DST01: 0.1−1.0 μm, DST02: 1.0−2.5 μm, DST03: 2.5−5.0 μm, and DST04: 5.0−10 μm) and sea salt (SSLT01: 0.2−1.0 μm, SSLT02: 1.0−3.0 μm, SSLT03: 3.0−10 μm, and SSLT04: 10−20 μm) (Su et al., 2022; Wu et al., 2019). Thus, the first two bins are assumed to belong to $PM_{2.5}$. Ammonium and nitrate are not available in most of these six models (except GISS-E2-1-MATRIX) and are thus not included in Eq.1.

2.2 Satellite-based total $PM_{2.5}$

We take satellite-based near-surface total $PM_{2.5}$ concentrations from the V4.CH.03 product of the Washington University Atmospheric Composition Analysis Group (Hammer et al., 2020). The dataset is constructed by combining multiple satellite products of AOD with simulations from a chemical transport model (GEOS-Chem) to predict $PM_{2.5}$, and then constraining these estimates by ground-level $PM_{2.5}$ monitoring. It provides the annual average $PM_{2.5}$ concentrations during 2000–2014 with a high spatial resolution of 0.01° × 0.01° (~1 × 1 km^2). Detailed data descriptions are provided elsewhere (van Donkelaar et al., 2019; van Donkelaar et al., 2016). Here the satellite-based total $PM_{2.5}$ data are re-gridded to 1° × 1° for model evaluation purposes.

https://doi.org/10.5194/egusphere-2023-2370
Preprint. Discussion started: 16 November 2023

2.3 Ground-based $PM_{2.5}$ components data

Since national-scale continuous measurements of near-surface $PM_{2.5}$ components are unavailable in China, we collect observational $PM_{2.5}$ component data from the literature. Our collected dataset includes 2469 component records of OC, BC, sulfate, nitrate, and ammonium nationwide (627, 66, 645, and 1131 records in western regions, Northeast China, North China, and Central and South China, respectively), as shown in Figure 1. Here a record represents one measured $PM_{2.5}$ component at the specific sample site and period. These records cover 30 provinces (including provinces and provincial-level municipalities) and multiple land use types (urban, rural, near the road, and industrial park, etc.). The dataset does not cover Ningxia, Guizhou, Heilongjiang, and Taiwan. A total of 472, 459, 518, 519, and 501 records are available for OC, BC, sulfate, nitrate, and ammonium over China, respectively. The site locations, sampling periods, data sources, and other information are summarized in the Supplement.

At a given site, the records are not continuous in time. These records cover varying sampling periods ranging from a few days to several years, although most are monthly data. We treat a record as seasonal if its data length is equal to or shorter than a season, or as annual when its data length is longer than 6 months. The records are not evenly scattered across years and are more available in later years in general. From 2000 to 2008, the numbers of records range from 50 to 150 per year, except for 2003 (207 records); while from 2009 to 2014, the numbers of records vary between 150 to 550 per year (Fig. S1). To compare with CMIP6 simulations, we calculate for each site the multi-year mean $PM_{2.5}$ component concentrations by averaging over the seasonal or annual observational records. If there are more than one sites in a given model grid cell, we average data from all sites in that grid cell. To consider the effect of interannual variability, we compute for each CMIP6 model the average and maximum of annual mean values over 2000–2014 from all grid cells with available observational data, and then compare with the multi-year averaged observations from these grid cells. As detailed in Section 5, the model biases are not caused by imperfect model-observation matching in time.

3 Evaluation of near-surface total $PM_{2.5}$

3.1 Spatial distribution

The spatial distribution of satellite-based annual mean total $PM_{2.5}$ concentrations (Fig. 2 p) exhibits high

https://doi.org/10.5194/egusphere-2023-2370
Preprint. Discussion started: 16 November 2023

values over populous and industrial North China (including Beijing, Tianjin, Hebei, Shandong, and Shanxi provinces, 52.6 μg m^{-3}) and eastern Sichuan (60.9 μg m^{-3}). Central and South China exhibits $PM_{2.5}$ concentrations (46.5 μg m^{-3}) lower than North China, due to lower emissions, higher vegetation coverage, better ventilation conditions and more precipitation. $PM_{2.5}$ concentrations are modest over dusty southern Xinjiang (33.6 μg m^{-3}). Low $PM_{2.5}$ concentrations (< 8 μg m^{-3}) are distributed over the plateaus or forested regions with small populations, such as Tibet and northern Heilongjiang. Overall, $PM_{2.5}$ concentrations in the south and coastal regions are lower than in the northern and inland regions.

Among the seven models that directly output total $PM_{2.5}$ concentrations (Fig. 2 a-g), GFDL-ESM4 and MPI-ESM-1-2-HAM show similar patterns and magnitudes to satellite data with small national average biases (–1.5% and –1.1%, respectively). Over the eastern regions (including Northeast China, North China, and Central and South China), all models exhibit spatially averaged negative biases ranging from by –47.9% to –3.3%. Nevertheless, the spatial pattern is well simulated by four models (GFDL-ESM4, GISS-E2-1-OMA, MIROC-ES2L, and MPI-ESM-1-2-HAM) ($R > 0.9$) with the maximum center over North China correctly reproduced. Over the western regions, four models (GFDL-ESM4, MRI-ESM2-0, NorESM2-LM, and NorESM2-MM) reproduce the maximum center over southern Xinjiang, although each of the seven models can underestimate or overestimate the peak values substantially.

For the seven models with total $PM_{2.5}$ derived from Eq.1, their simulated $PM_{2.5}$ concentrations underestimate the satellite-based data by –65.5% to –48.0% averaged over the country (Fig.2 h-n). The negative biases are in part because nitrate and ammonium are not included (10.4–17.2% and 10.1–11.1% of $PM_{2.5}$ are nitrate and ammonium in the models that do contain them). Over the eastern regions, HadGEM3-GC31-LL and UKESM1-0-LL exhibit the least underestimation, and they also capture the observed maximum center over North China. Five of these seven models do not reproduce the $PM_{2.5}$ peaks over dusty regions in the west, pointing to model deficiencies in dust simulations (Zhao et al., 2022).

3.2 Trend and interannual variability

Over the eastern regions (Northeast China, North China, and Central and South China), data from satellite (0.72 μg m^{-3} yr^{-1}) and all models (0.32–1.14 μg m^{-3} yr^{-1}) exhibit significant increases (p-value < 0.05)

https://doi.org/10.5194/egusphere-2023-2370
Preprint. Discussion started: 16 November 2023

in annual mean total $PM_{2.5}$ concentrations over 2000–2014, with temporal correlation between 0.63 and 0.87 (Fig. 3 a and Table S2). GFDL-ESM4 and MPI-ESM1-2-HAM exhibit annual average $PM_{2.5}$ concentrations and trends similar to the satellite data since 2004. Regionally, the fourteen models capture the interannual variations of satellite $PM_{2.5}$ over Northeast China ($R > 0.9$) and North China ($R > 0.8$) (Fig. 4). The temporal consistency reflects that the models capture the temporal changes in anthropogenic emissions over these polluted regions, although the models might not align with natural (meteorology-driven) variability.

Over the western regions where natural dust dominates the aerosol loadings, satellite-based $PM_{2.5}$ concentrations experience no significant trend over 2000–2014, whereas 11 models increase significantly ranging from 0.10–0.28 μg m^{-3} yr^{-1}) (Fig. 3 b). The notable decline over 2000–2005 in satellite data (–1.12 μg m^{-3} yr^{-1}), which reaches 90% confidence level but no 95%, is not captured by any model. Over 2000–2014, NorESM2-LM, NorESM2-MM, and MPI-ESM-1-2-HAM show large interannual variations whereas other models do not. The models do not align with the yearly changes found in the satellite data, with modestly positive, low or even negative correlation coefficients (–0.6 to 0.6, Fig. 4). The inaccuracy in aerosol trend and variability might exert erroneous forcing upon the climate system.

4 Evaluation of near-surface $PM_{2.5}$ components

4.1 Organic carbon and black carbon

Ground-based observations of carbonaceous aerosols (OC and BC) are mostly available in the eastern regions. The national average multi-year mean observed OC concentration reaches 15.9 μg m^{-3}. Observed OC concentrations peak over North China (> 25 μg m^{-3}) and are also high over Central and South China (5–25 μg m^{-3}) (Fig. 5 a). The national average of the 14-model mean (6.5 μg m^{-3}, NMB = –59.0%), which are spatially coincidently sampled with the ground-based observations, severely underestimates the observations, especially over parts of North China with the bias reaching –40 μg m^{-3} (Fig. 5 b). Nevertheless, the spatial pattern of OC observations is captured by the 14-model mean modestly well with a correlation coefficient of 0.51. Further, a negative bias exceeding –50% occurs in 11 models, even though they can simulate the spatial pattern moderately well (R ranges from 0.40 to 0.58, Fig. S2). The discrepancy of OC between models peaks over North China and eastern Sichuan, as shown in Figure 5 c.

https://doi.org/10.5194/egusphere-2023-2370
Preprint. Discussion started: 16 November 2023

The national average multi-year mean observed BC concentration is 4.3 μg m^{-3}. Observed BC concentrations are high (> 10 μg m^{-3}) over parts of North China with mining and other heavy industries, such as Hebei and Shanxi province (Fig. 5 d). However, the 14-model mean (3 μg m^{-3}) does not capture the spatial pattern very well (R = 0.39) and it underestimates the observations (NMB = –27.2%). The 14-model mean presents the largest negative bias over Shanxi (–15.2 μg m^{-3}) and the greatest positive bias over Shandong (3.9 μg m^{-3}, Fig. 5 e); both provinces are in North China. Twelve of the 14 models underestimate the BC observations (by –47.9% to –12.1% for national average), whereas two models (HadGEM3-GC31-LL and UKESM1-0-LL) exhibit positive biases (by 21.1% and 26.2%, respectively) (Fig. 6 and Fig. S3). Most models produce high concentrations of BC over the whole North China, including Beijing and Shandong that exhibit relatively low observational values.

The underestimation of carbonaceous aerosol concentrations might be associated with anthropogenic emissions, chemical mechanisms, and meteorological conditions. The CEDS emission data (ver. 2016-07-26) used in CMIP6 historical simulations are overestimated in China. However, the positive bias in emissions cannot explain the model underestimation of OC and BC concentrations. Instead, the model inadequacies in chemical processes (e.g. using simplified aerosols and chemistry schemes, which tends to underestimate aerosol formation) (Turnock et al., 2020), might lead to underestimated secondary organic aerosols (SOA) concentrations, especially over Central and South China (Chen et al., 2016).

Meteorological conditions, including temperature, precipitation and surface wind simulations, have critical impacts on local aerosol concentrations. Temperature simulations over the eastern regions of China by CMIP6 models are very close to the observed data (Yang et al., 2021). Over the western regions, a notable warm bias over Xinjiang may contribute to higher boundary layer height and stronger vertical mixing, partly explaining the underestimation of OC and BC concentrations near the surface (Fig. 5); whereas the pronounced cold bias over the Tibetan Plateau might contribute to overestimated near-surface aerosol concentrations over there. Precipitation affects aerosol concentrations through wet scavenging; and it is overestimated (wet bias) in CMIP6 models over North China and Northeast China but close to observations over Central and South China (Yang et al., 2021). The model performance in precipitation may partly explain the more severe underestimation of OC concentrations over North China than over Central and South China. But the overestimation of BC over North China suggests that other

https://doi.org/10.5194/egusphere-2023-2370
Preprint. Discussion started: 16 November 2023

factors offset the influence of local wet bias. Over the western regions, most models exhibit wet bias, except over northern Xinjiang where local temperature (warm bias) and precipitation (dry bias) have opposite effects on near-surface aerosol concentrations. Furthermore, the overall underestimation of surface wind speed over China in CMIP6 (Wu et al., 2020) is conducive to the accumulation of near-surface aerosol concentrations around the anthropogenic emission source regions, which may induce a negative contribution to the underestimation of OC and BC concentrations.

4.2 Sulfate, nitrate and ammonium

This section evaluates the model performance of secondary inorganic aerosols (sulfate, nitrate, and ammonium; SIOA). The national average multi-year mean of observed sulfate concentrations reaches 14.6 μg m^{-3}, the second largest value among the five $PM_{2.5}$ components (following OC). The observed sulfate concentrations exceed 15 μg m^{-3} over most of North China and eastern Sichuan, as well as cities over Xinjiang with large population and petroleum industry (Fig. 5 g). The 14-model mean, whose national average is 9.3 μg m^{-3}, has the greatest underestimation over North China and Xinjiang (Fig. 5 h). The 14-model mean agrees modestly well with the observations in spatial pattern (R = 0.57). Among the 14 models, the national average model biases range from –66.1% (GISS-E2-1-OMA) to 24.5% (MRI-ESM2-0); and five models better capture the observed spatial pattern with correlation coefficients exceeding 0.6 (Fig. 6). The cross-model discrepancy in sulfate (2 μg m^{-3} in national average) is larger than those for the other four components (0.4–0.9 μg m^{-3}), particularly over Central and South China (Fig. 5 i).

The national average multi-year mean of observational nitrate concentrations is 8.7 μg m^{-3}. The observed spatial pattern of nitrate is similar to sulfate, with high values over North China, eastern Sichuan and populous cities of Xinjiang (Fig. 5 j). Only four models (GFDL-ESM4, GISS-E2-1-OMA, GISS-E2-1-MATRIX, and EC-Earth3-AerChem) include nitrate simulations. The 4-model mean has a national average of 5.5 μg m^{-3}, with a NMB of –36.5%; but it captures the observed spatial pattern very well with a correlation coefficient reaching 0.7. All the four models exhibit negative NMBs ranging from –41.4% to –25.4%; they reproduce high values over the eastern regions but have underestimation over Xinjiang (Fig. S5).

https://doi.org/10.5194/egusphere-2023-2370
Preprint. Discussion started: 16 November 2023

The observed multi-year mean ammonium concentrations have a national average value of 6.7 μg m^{-3}. The observational values peak over North China (> 10 μg m^{-3}), particularly over the agricultural regions from which ammonia emissions are the greatest (Fig. 5 m). Five models perform ammonium simulations. The 5-model mean, with a national average of 3.4 μg m^{-3}, has negative and positive biases between –12.2 and 1.5 μg m^{-3} at different locations (Fig. 5 n). The 5-model mean captures the observed spatial pattern of ammonium (R = 0.74) better than for other components (R = 0.39–0.70). The five models exhibit varying performances in magnitude and spatial pattern. The NMBs range from –89.0% to –13.6% across these models. Four models simulate the spatial patterns of ammonium well with high correlation coefficients between 0.67 to 0.76, although the spatial agreement is poor for CESM2-WACCM (R = 0.21).

Emissions, meteorological conditions and chemical processes affect the formation and loss of secondary inorganic aerosols. As explained in Sect. 4.1, the potentially overestimated CEDS emissions over China, the cold bias over the Tibetan Plateau, and the dry bias over northern Xinjiang tend to overestimate aerosol concentrations, which are in contrast with the negative model biases over the respective regions. On the other hand, the warm bias over northern Xinjiang and the wet bias over North China and Northeast China are in line with the underestimation of aerosol concentrations. Furthermore, the formation of nitrate from nitric acid depends on the amount of residual ammonia left from the formation of ammonium sulfate. Over the regions where ammonia is not sufficient to neutralize both nitric acid and sulfuric acid (such as Shanxi and Shandong), decreased sulfate formation might promote nitrate formation with the released ammonium (Zhai et al., 2019; Zhai et al., 2021). This partly explains why the underestimation of nitrate simulations is less than sulfate over these regions.

5 Discussion

Over the eastern regions, the concentrations of total $PM_{2.5}$ and its five components are underestimated by the 14 models in general. The slight underestimation of three models (GFDL-ESM4, MPI-ESM-1-2-HAM, and MRI-ESM2-0) can be traced to positive biases in sulfate simulations partly offsetting the negative biases in OC and BC. Over the western regions, most models underestimate the total $PM_{2.5}$ concentrations dominated by dust aerosols, whereas three models (GFDL-ESM4, NorESM2-LM, and NorESM2-MM) produce overly high values over Xinjiang due to overestimated dust concentrations.

https://doi.org/10.5194/egusphere-2023-2370
Preprint. Discussion started: 16 November 2023

Meanwhile, all models underestimate the five $PM_{2.5}$ components over the west.

Figure 7 shows little difference between the maximum and average annual concentrations over 2000–2014 for national mean $PM_{2.5}$ components simulated by individual models. Furthermore, we average over all seasonal and annual observational records to compare with annual mean model results. A test using the seasonal (annual) model results to match seasonal (annual) observational records shows very similar comparison results (Fig. S6). These tests suggest that the model underestimation cannot be attributed to imperfect temporal matching between models and observations or the potential mis-phase (or variability) in models.

Among the five $PM_{2.5}$ components evaluated, absorbing aerosol (BC) and four scattering aerosols (OC, sulfate, nitrate, and ammonium) have opposite direct radiative forcing at the top of atmosphere (TOA). The underestimation of BC is less than for the other four scattering aerosols. If this difference persists in the troposphere, the underestimated $PM_{2.5}$ components might cause an underestimation of negative radiative forcing at TOA. The underestimation of BC and scatter aerosols might result in more solar radiation reaching the ground (Chen et al., 2022; Tang et al., 2022). This is consistent with the overestimation of maximum daily maximum temperature over the eastern regions (Zhu et al., 2020), likely serving as a positive feedback between negative aerosol biases and overestimated surface temperature.

The spatial biases in aerosols might also serve as an important limiting factor for the performance of meteorological/climate simulations. The observed $PM_{2.5}$ and its five components are characterized by high concentrations over the east and low values over the west (except northern Xinjiang). In a few models, the large overestimation of $PM_{2.5}$ over Xinjiang of the west (dominated by dust) with underestimated $PM_{2.5}$ (dominated by anthropogenic aerosols) over the east might exert an incorrect west-east asymmetric climate forcing. The spatial pattern of resulting climate response might include cold-warm biases of surface temperature (cold bias over the west and warm bias over the east). The difference in the spatial pattern of model bias between BC and scattering aerosols might have additional impacts on the climate. Future work is needed to examine how the model errors in $PM_{2.5}$ and its components might affect climate simulations through aerosol-climate feedback.

https://doi.org/10.5194/egusphere-2023-2370
Preprint. Discussion started: 16 November 2023

6 Summary

In this study, we evaluate the performance of 14 CMIP6 ESMs in simulating total near-surface $PM_{2.5}$ and its five components over China during 2000–2014, and discuss the likely causes for model errors, and their climate implications. Our assessment helps to understand the capability of the current-generation models in the simulation of aerosols and aerosol-climate interactions, towards further improvement of climate predictions and projections. Our findings are summarized as follows:

(1) Twelve of the 14 CMIP6 models tend to underestimate the total $PM_{2.5}$ concentrations over China (NMB = –65.5% to –1.1%) and the other two models overestimate them (NMB = 17.0%–39.2%), as compared to a satellite-based dataset. The seven models that output total $PM_{2.5}$ concentrations exhibit underestimation between –47.9% and –3.3% over the eastern regions, although four of them capture the observed spatial pattern ($R > 0.9$). Over the western regions, four of these seven models reproduce the maximum center over southern Xinjiang. The seven models, for which we calculate the total $PM_{2.5}$ concentrations from outputted components, underestimate the observed $PM_{2.5}$ by –65.5% to –48.0% averaged over the country, in part due to missing nitrate and ammonium in the models.

(2) Over the eastern regions, all models simulate significant increasing trends of total $PM_{2.5}$ (0.32–1.14 $\mu g\ m^{-3}\ yr^{-1}$) over 2000–2014 that are close to satellite-based data (0.72 $\mu g\ m^{-3}\ yr^{-1}$). The models also capture the interannual variability of satellite $PM_{2.5}$ over Northeast China and North China. Over the western regions, 11 models simulate growing $PM_{2.5}$ concentrations at rates of 0.10–0.28 $\mu g\ m^{-3}\ yr^{-1}$, in contrast to no significant trends in satellite data.

(3) The 14-model mean captures the spatial pattern of observed OC modestly well ($R = 0.51$), but it exhibits severe underestimation nationwide (NMB = –59.0%), with negative biases exceeding –50% in 11 models. The 14-model mean shows a poor capability in capturing the BC spatial pattern ($R = 0.39$), and it also underestimates the BC observations (NMB = –27.2%). Two models exhibit positive biases in BC, while the other 12 models exhibit negative biases.

(4) Fourteen, four and five models output the sulfate, nitrate, and ammonium, respectively. The 14-model mean of sulfate exhibits modest spatial correlation and bias ($R = 0.57$, NMB = –36.5%); and there exist large discrepancies among these models, with biases ranging from –66.1% to 24.5%. The 4-model

https://doi.org/10.5194/egusphere-2023-2370
Preprint. Discussion started: 16 November 2023

mean of nitrate captures the spatial pattern well (R = 0.7), although it still underestimates concentrations nationwide (NMB = –36.5%). The 5-model mean of ammonium has the best performance in reproducing the spatial pattern (R = 0.74) but with a negative bias in magnitudes (NMB = –46.5%).

(5) The overall underestimation of $PM_{2.5}$ and its components are associated with imperfectness in emissions as input, modeled meteorology and chemistry. The underestimated $PM_{2.5}$ and its components might cause an overall underestimated cooling effect at TOA and stronger warming at the surface in the models. The model performance in spatial pattern differs between BC and scattering aerosols; and a few models also exhibit strong positive biases over the west (associated with dust) but negative biases over the east. Together, the errors in spatial pattern might have additional consequences for the modeled climate. Further studies are warranted to quantify how model errors in the magnitude and spatial pattern of aerosols affect the regional and global climate, for example, through the Regional Aerosol Model Intercomparison Project (RAMIP) (Wilcox et al., 2022).

As a final note, the underestimated aerosol concentrations might also affect the ozone simulation through radiative or heterogeneous chemical processes (Jacob, 2000; Lin et al., 2012; Li et al., 2019) In addition, as CMIP6 models are also used to study the health impacts of aerosols (Xu et al., 2022; Shim et al., 2021), the aerosol underestimation needs to be corrected to allow a more reliable estimate of health consequences.

Data availability

CMIP6 data are available on the Earth System Grid Federation (ESGF) and can be freely downloaded via the website interface https://esgf-data.dkrz.de/search/cmip6-dkrz/ (last access: 8 September 2020, WCRP, 2020). Satellite-derived surface $PM_{2.5}$ concentration products can be accessed from the Washington University Atmospheric Composition Analysis Group website as version V4.CH.03 at https://sites.wustl.edu/acag/datasets/surface-pm2-5/. Observational data used in this paper are provided in the SI, with raw data available upon request to the corresponding author Jintai Lin (linjt@pku.edu.cn).

Author contributions

JL led the study. FR and JL designed the study, analyzed the results, and wrote the paper. CX provided

https://doi.org/10.5194/egusphere-2023-2370
Preprint. Discussion started: 16 November 2023

the map data of four regions in China. JA collected observation data of $PM_{2.5}$ components from the literature. JW helped to analyze the evaluation results. RM, AD and MH provided satellite-derived data of total $PM_{2.5}$. ST performed UKESM1-0-LL and HadGEM3-GC31-LL simulations. NO performed MRI-ESM2-0 simulations. JZ performed BCC-ESM1 simulations. SB and KT performed GISS-E2-1-OMA and GISS-E2-1-MATRIX simulations. ØS performed NorESM2-LM and NorESM2-MM simulations. PN performed CNRM-ESM2-1 simulations. DN performed MPI-ESM1-2-HAM simulations. GS performed CESM2-WACCM simulations. TN and PS performed EC-Earth3-AerChem simulations. LH performed GFDL-ESM4 simulations. TT performed MIROC-ES2L simulations. All authors commented on the manuscript.

Competing interests

The authors declare that they have no conflict of interests.

Financial support

Jintai Lin and Fangxuan Ren have been supported by the National Natural Science Foundation of China (grant no. 42075175) and the second Tibetan Plateau Scientific Expedition and Research Program 525 (grant no. 2019QZKK0604). Naga Oshima has been supported by the Environment Research and Technology Development Fund (grant nos. JPMEERF20202003 and JPMEERF20232001) of the Environmental Restoration and Conservation Agency provided by Ministry of the Environment of Japan, the Arctic Challenge for Sustainability II (ArCS II, grant no. JPMXD1420318865), and the Global Environmental Research Coordination System from Ministry of the Environment, Japan (grant no. MLIT2253). David Neubauer has been supported by the European Union's Horizon 2020 research and innovation programme project (FORCeS, grant no. 821205). Randall Martin has been supported by NASA (grant no. 80NSSC21K0508).

Reference

Allen, R. J. and Landuyt, W.: The vertical distribution of black carbon in CMIP5 models: Comparison to observations and the importance of convective transport, J. Geophys. Res. Atmos., 119, 4808-4835, https://doi.org/10.1002/2014JD021595, 2014.

Allen, R. J., Norris, J. R., and Wild, M.: Evaluation of multidecadal variability in CMIP5 surface solar radiation and inferred underestimation of aerosol direct effects over Europe, China, Japan, and India, J. Geophys. Res. Atmos., 118, 6311-6336, https://doi.org/10.1002/jgrd.50426, 2013.

Bauer, S. E., Tsigaridis, K., Faluvegi, G., Kelley, M., Lo, K. K., Miller, R. L., Nazarenko, L., Schmidt,

https://doi.org/10.5194/egusphere-2023-2370
Preprint. Discussion started: 16 November 2023

G. A., and Wu, J.: Historical (1850–2014) Aerosol Evolution and Role on Climate Forcing Using the GISS ModelE2.1 Contribution to CMIP6, J. Adv. Model. Earth Syst., 12, e2019MS001978, https://doi.org/10.1029/2019MS001978, 2020.

Buchard, V., da Silva, A. M., Randles, C. A., Colarco, P., Ferrare, R., Hair, J., Hostetler, C., Tackett, J., and Winker, D.: Evaluation of the surface $PM_{2.5}$ in Version 1 of the NASA MERRA Aerosol Reanalysis over the United States, Atmos. Environ., 125, 100-111, https://doi.org/10.1016/j.atmosenv.2015.11.004, 2016.

Bürki, C., Reggente, M., Dillner, A. M., Hand, J. L., Shaw, S. L., and Takahama, S.: Analysis of functional groups in atmospheric aerosols by infrared spectroscopy: method development for probabilistic modeling of organic carbon and organic matter concentrations, Atmos. Meas. Tech., 13, 1517-1538, https://doi.org/10.5194/amt-13-1517-2020, 2020.

Carslaw, K. S., Lee, L. A., Reddington, C. L., Pringle, K. J., Rap, A., Forster, P. M., Mann, G. W., Spracklen, D. V., Woodhouse, M. T., Regayre, L. A., and Pierce, J. R.: Large contribution of natural aerosols to uncertainty in indirect forcing, Nature, 503, 67-71, https://doi.org/10.1038/nature12674, 2013.

Chen, D., Liao, H., Yang, Y., Chen, L., Zhao, D., and Ding, D.: Simulated impacts of vertical distributions of black carbon aerosol on meteorology and $PM_{2.5}$ concentrations in Beijing during severe haze events, Atmos. Chem. Phys., 22, 1825-1844, https://doi.org/10.5194/acp-22-1825-2022, 2022.

Chen, Y., Li, J., Lee, W., Diner, D., Garay, M., Jiang, J., Wang, Y., Yu, J., and Kalashnikova, O.: Evaluation of sea salt aerosols in climate systems: global climate modeling and observation-based analyses, Environ. Res. Lett., 15, 034047, https://doi.org/10.1088/1748-9326/ab751c, 2020.

Chen, Z., Liu, J. F., Tao, W., and Tao, S.: Spatiotemporal distribution and source attribution of SOA in China, Huan Jing Ke Xue, 37, 2815-2822, https://doi.org/10.13227/j.hjkx.2016.08.001, 2016.

Cherian, R. and Quaas, J.: Trends in AOD, Clouds, and Cloud Radiative Effects in Satellite Data and CMIP5 and CMIP6 Model Simulations Over Aerosol Source Regions, Geophys. Res. Lett., 47, e2020GL087132, https://doi.org/10.1029/2020GL087132, 2020.

Evan, A. T., Flamant, C., Gaetani, M., and Guichard, F.: The past, present and future of African dust, Nature, 531, 493-495, https://doi.org/10.1038/nature17149 2016.

Eyring, V., Bony, S., Meehl, G. A., Senior, C. A., Stevens, B., Stouffer, R. J., and Taylor, K. E.: Overview of the Coupled Model Intercomparison Project Phase 6 (CMIP6) experimental design and organization, Geosci. Model Dev., 9, 1937-1958, https://doi.org/10.5194/gmd-9-1937-2016, 2016.

Fan, T., Zhao, C., Dong, X., Liu, X., Yang, X., Zhang, F., Shi, C., Wang, Y., and Wu, F.: Quantify contribution of aerosol errors to cloud fraction biases in CMIP5 Atmospheric Model Intercomparison Project simulations, Int. J. Climatol., 38, 3140-3156, https://doi.org/10.1002/joc.5490, 2018a.

Fan, T., Liu, X., Ma, P.-L., Zhang, Q., Li, Z., Jiang, Y., Zhang, F., Zhao, C., Yang, X., Wu, F., and Wang, Y.: Emission or atmospheric processes? An attempt to attribute the source of large bias of aerosols in eastern China simulated by global climate models, Atmos. Chem. Phys., 18, 1395-1417,

https://doi.org/10.5194/egusphere-2023-2370
Preprint. Discussion started: 16 November 2023

https://doi.org/10.5194/acp-18-1395-2018, 2018b.

Feng, L., Smith, S. J., Braun, C., Crippa, M., Gidden, M. J., Hoesly, R., Klimont, Z., van Marle, M., van den Berg, M., and van der Werf, G. R.: The generation of gridded emissions data for CMIP6, Geosci. Model Dev., 13, 461-482, https://doi.org/10.5194/gmd-13-461-2020, 2020.

Hammer, M. S., van Donkelaar, A., Li, C., Lyapustin, A., Sayer, A. M., Hsu, N. C., Levy, R. C., Garay, M. J., Kalashnikova, O. V., Kahn, R. A., Brauer, M., Apte, J. S., Henze, D. K., Zhang, L., Zhang, Q., Ford, B., Pierce, J. R., and Martin, R. V.: Global Estimates and Long-Term Trends of Fine Particulate Matter Concentrations (1998–2018), Environ. Sci. Technol., 54, 7879-7890, https://doi.org/10.1021/acs.est.0c01764, 2020.

Hoesly, R. M., Smith, S. J., Feng, L., Klimont, Z., Janssens-Maenhout, G., Pitkanen, T., Seibert, J. J., Vu, L., Andres, R. J., Bolt, R. M., Bond, T. C., Dawidowski, L., Kholod, N., Kurokawa, J. I., Li, M., Liu, L., Lu, Z., Moura, M. C. P., O'Rourke, P. R., and Zhang, Q.: Historical (1750–2014) anthropogenic emissions of reactive gases and aerosols from the Community Emissions Data System (CEDS), Geosci. Model Dev., 11, 369-408, https://doi.org/10.5194/gmd-11-369-2018, 2018.

Huang, Y., Shen, H., Chen, Y., Zhong, Q., Chen, H., Wang, R., Shen, G., Liu, J., Li, B., and Tao, S.: Global organic carbon emissions from primary sources from 1960 to 2009, Atmos. Environ., 122, 505-512, https://doi.org/10.1016/j.atmosenv.2015.10.017, 2015.

Jacob, D. J.: Heterogeneous chemistry and tropospheric ozone, Atmos. Environ., 34, 2131-2159, https://doi.org/10.1016/S1352-2310(99)00462-8, 2000.

Li, K., Jacob, D. J., Liao, H., Zhu, J., Shah, V., Shen, L., Bates, K. H., Zhang, Q., and Zhai, S.: A two-pollutant strategy for improving ozone and particulate air quality in China, Nat. Geosci., 12, 906-910, https://doi.org/10.1038/s41561-019-0464-x, 2019.

Li, R., Ma, X., Xiong, F., Jia, H., Sha, T., and Tian, R.: Comparisons and evaluation of aerosol burden and optical depth in CMIP5 simulations over East Asia, J. Atmos. Solar-Terr. Phys., 206, 105315, https://doi.org/10.1016/j.jastp.2020.105315, 2020.

Li, X., Liu, Y., Wang, M., Jiang, Y., and Dong, X.: Assessment of the Coupled Model Intercomparison Project phase 6 (CMIP6) Model performance in simulating the spatial-temporal variation of aerosol optical depth over Eastern Central China, Atmos. Res., 261, 105747, https://doi.org/10.1016/j.atmosres.2021.105747, 2021.

Lin, J., Tong, D., Davis, S., Ni, R., Tan, X., Pan, D., Zhao, H., Lu, Z., Streets, D., Feng, T., Zhang, Q., Yan, Y., Hu, Y., Li, J., Liu, Z., Jiang, X., Geng, G., He, K., Huang, Y., and Guan, D.: Global climate forcing of aerosols embodied in international trade, Nat. Geosci., 9, 790-794, https://doi.org/10.1038/ngeo2798, 2016.

Lin, J. T., Liu, Z., Zhang, Q., Liu, H., Mao, J., and Zhuang, G.: Modeling uncertainties for tropospheric nitrogen dioxide columns affecting satellite-based inverse modeling of nitrogen oxides emissions, Atmos. Chem. Phys., 12, 12255-12275, https://doi.org/10.5194/acp-12-12255-2012, 2012.

https://doi.org/10.5194/egusphere-2023-2370
Preprint. Discussion started: 16 November 2023

Liu, R.-J. and Liao, H.: Assessment of aerosol effective radiative forcing and surface air temperature response over eastern China in CMIP5 models, Atmos. Oceanic Sci. Lett., 10, 228-234, https://doi.org/10.1080/16742834.2017.1301188, 2017.

Ma, X., Yan, P., Zhao, T., Jia, X., Jiao, J., Ma, Q., Wu, D., Shu, Z., Sun, X., and Habtemicheal, B. A.: Evaluations of Surface PM10 Concentration and Chemical Compositions in MERRA-2 Aerosol Reanalysis over Central and Eastern China, Remote Sens., 13, 1317, https://doi.org/10.3390/rs13071317, 2021.

Mahesh, B., Rama, B. V., Spandana, B., Sarma, M. S. S. R. K. N., Niranjan, K., and Sreekanth, V.: Evaluation of MERRAero $PM_{2.5}$ over Indian cities, Adv. Space Res., 64, 328-334, https://doi.org/10.1016/j.asr.2019.04.026, 2019.

McDuffie, E. E., Smith, S. J., O'Rourke, P., Tibrewal, K., Venkataraman, C., Marais, E. A., Zheng, B., Crippa, M., Brauer, M., and Martin, R. V.: A global anthropogenic emission inventory of atmospheric pollutants from sector- and fuel-specific sources (1970–2017): an application of the Community Emissions Data System (CEDS), Earth Syst. Sci. Data, 12, 3413-3442, https://doi.org/10.5194/essd-12-3413-2020, 2020.

Michou, M., Nabat, P., Saint-Martin, D., Bock, J., Decharme, B., Mallet, M., Roehrig, R., Séférian, R., Sénési, S., and Voldoire, A.: Present-Day and Historical Aerosol and Ozone Characteristics in CNRM CMIP6 Simulations, J. Adv. Model. Earth Syst., 12, e2019MS001816, https://doi.org/10.1029/2019MS001816, 2020.

Mortier, A., Gliß, J., Schulz, M., Aas, W., Andrews, E., Bian, H., Chin, M., Ginoux, P., Hand, J., Holben, B., Zhang, H., Kipling, Z., Kirkevåg, A., Laj, P., Lurton, T., Myhre, G., Neubauer, D., Olivié, D., von Salzen, K., Skeie, R. B., Takemura, T., and Tilmes, S.: Evaluation of climate model aerosol trends with ground-based observations over the last 2 decades – an AeroCom and CMIP6 analysis, Atmos. Chem. Phys., 20, 13355-13378, https://doi.org/10.5194/acp-20-13355-2020, 2020.

Mulcahy, J. P., Johnson, C., Jones, C. G., Povey, A. C., Scott, C. E., Sellar, A., Turnock, S. T., Woodhouse, M. T., Abraham, N. L., Andrews, M. B., Bellouin, N., Browse, J., Carslaw, K. S., Dalvi, M., Folberth, G. A., Glover, M., Grosvenor, D. P., Hardacre, C., Hill, R., Johnson, B., Jones, A., Kipling, Z., Mann, G., Mollard, J., O'Connor, F. M., Palmiéri, J., Reddington, C., Rumbold, S. T., Richardson, M., Schutgens, N. A. J., Stier, P., Stringer, M., Tang, Y., Walton, J., Woodward, S., and Yool, A.: Description and evaluation of aerosol in UKESM1 and HadGEM3-GC3.1 CMIP6 historical simulations, Geosci. Model Dev., 13, 6383-6423, https://doi.org/10.5194/gmd-13-6383-2020, 2020.

Park, H., Chung, C. E., Ekman, A. M. L., and Choi, J.-O.: Evaluation of ACCMIP simulated fine-mode AOD and its implication for aerosol direct forcing, Asia Pac. J. Atmos. Sci., 50, 377-390, https://doi.org/10.1007/s13143-014-0025-6, 2014.

Paulot, F., Paynter, D., Ginoux, P., Naik, V., and Horowitz, L. W.: Changes in the aerosol direct radiative forcing from 2001 to 2015: observational constraints and regional mechanisms, Atmos. Chem. Phys., 18, 13265-13281, https://doi.org/10.5194/acp-18-13265-2018, 2018.

https://doi.org/10.5194/egusphere-2023-2370
Preprint. Discussion started: 16 November 2023

559 Pu, B. and Ginoux, P.: How reliable are CMIP5 models in simulating dust optical depth?, Atmos. Chem.
560 Phys., 18, 12491-12510, https://doi.org/10.5194/acp-18-12491-2018, 2018.

561 Seinfeld, J. H., Bretherton, C., Carslaw, K. S., Coe, H., DeMott, P. J., Dunlea, E. J., Feingold, G., Ghan,
562 S., Guenther, A. B., Kahn, R., Kraucunas, I., Kreidenweis, S. M., Molina, M. J., Nenes, A., Penner, J. E.,
563 Prather, K. A., Ramanathan, V., Ramaswamy, V., Rasch, P. J., Ravishankara, A. R., Rosenfeld, D.,
564 Stephens, G., and Wood, R.: Improving our fundamental understanding of the role of aerosol−cloud
565 interactions in the climate system, P. Natl. Acad. Sci. USA, 113, 5781-5790,
566 https://doi.org/10.1073/pnas.1514043113, 2016.

567 Shim, S., Sung, H., Kwon, S., Kim, J., Lee, J., Sun, M., Song, J., Ha, J., Byun, Y., Kim, Y., Turnock, S.
568 T., Stevenson, D. S., Allen, R. J., O'Connor, F. M., Teixeira, J. C., Williams, J., Johnson, B., Keeble, J.,
569 Mulcahy, J., and Zeng, G.: Regional Features of Long-Term Exposure to $PM_{2.5}$ Air Quality over Asia
570 under SSP Scenarios Based on CMIP6 Models, Int. J. Environ. Res. Public Health, 18, 6817,
571 https://doi.org/10.3390/ijerph18136817, 2021.

572 Sockol, A. and Small Griswold, J. D.: Intercomparison between CMIP5 model and MODIS satellite-
573 retrieved data of aerosol optical depth, cloud fraction, and cloud-aerosol interactions, Earth Space Sci.,
574 4, 485-505, https://doi.org/10.1002/2017EA000288, 2017.

575 Su, X., Wu, T., Zhang, J., Zhang, Y., Jin, J., Zhou, Q., Zhang, F., Liu, Y., Zhou, Y., Zhang, L., Turnock,
576 S. T., and Furtado, K.: Present-Day $PM_{2.5}$ over Asia: Simulation and Uncertainty in CMIP6 ESMs, J.
577 Meteorol. Res., 36, 429-449, https://doi.org/10.1007/s13351-022-1202-7, 2022.

578 Tang, Z., Tian, J., Zhang, Y., Zhang, X., Zhang, J., Ma, N., Li, X., and Song, P.: Anthropogenic aerosols
579 dominated the decreased solar radiation in eastern China over the last five decades, J. Clean. Prod., 380,
580 135150, https://doi.org/10.1016/j.jclepro.2022.135150, 2022.

581 Tao, S., Ru, M. Y., Du, W., Zhu, X., Zhong, Q. R., Li, B. G., Shen, G. F., Pan, X. L., Meng, W. J., Chen,
582 Y. L., Shen, H. Z., Lin, N., Su, S., Zhuo, S. J., Huang, T. B., Xu, Y., Yun, X., Liu, J. F., Wang, X. L., Liu,
583 W. X., Cheng, H. F., and Zhu, D. Q.: Quantifying the rural residential energy transition in China from
584 1992 to 2012 through a representative national survey, Nat. Energy, 3, 567-573,
585 https://doi.org/10.1038/s41560-018-0158-4, 2018.

586 Turnock, S. T., Allen, R. J., Andrews, M., Bauer, S. E., Deushi, M., Emmons, L., Good, P., Horowitz, L.,
587 John, J. G., Michou, M., Nabat, P., Naik, V., Neubauer, D., O'Connor, F. M., Olivié, D., Oshima, N.,
588 Schulz, M., Sellar, A., Shim, S., Takemura, T., Tilmes, S., Tsigaridis, K., Wu, T., and Zhang, J.: Historical
589 and future changes in air pollutants from CMIP6 models, Atmos. Chem. Phys., 20, 14547-14579,
590 https://doi.org/10.5194/acp-20-14547-2020, 2020.

591 van Donkelaar, A., Martin, R. V., Li, C., and Burnett, R. T.: Regional Estimates of Chemical Composition
592 of Fine Particulate Matter Using a Combined Geoscience-Statistical Method with Information from
593 Satellites, Models, and Monitors, Environ. Sci. Technol., 53, 2595-2611,
594 https://doi.org/10.1021/acs.est.8b06392, 2019.

595 van Donkelaar, A., Martin, R. V., Brauer, M., Hsu, N. C., Kahn, R. A., Levy, R. C., Lyapustin, A., Sayer,

https://doi.org/10.5194/egusphere-2023-2370
Preprint. Discussion started: 16 November 2023

A. M., and Winker, D. M.: Global Estimates of Fine Particulate Matter using a Combined Geophysical-Statistical Method with Information from Satellites, Models, and Monitors, Environ. Sci. Technol., 50, 3762-3772, https://doi.org/10.1021/acs.est.5b05833, 2016.

Wang, R., Tao, S., Shen, H., Huang, Y., Chen, H., Balkanski, Y., Boucher, O., Ciais, P., Shen, G., Li, W., Zhang, Y., Chen, Y., Lin, N., Su, S., Li, B., Liu, J., and Liu, W.: Trend in Global Black Carbon Emissions from 1960 to 2007, Environ. Sci. Technol., 48, 6780-6787, https://doi.org/10.1021/es5021422, 2014.

Wang, Z., Lin, L., Xu, Y., Che, H., Zhang, X., Zhang, H., Dong, W., Wang, C., Gui, K., and Xie, B.: Incorrect Asian aerosols affecting the attribution and projection of regional climate change in CMIP6 models, NPJ Clim. Atmos. Sci., 4, 2, https://doi.org/10.1038/s41612-020-00159-2, 2021.

Wilcox, L. J., Allen, R. J., Samset, B. H., Bollasina, M. A., Griffiths, P. T., Keeble, J. M., Lund, M. T., Makkonen, R., Merikanto, J., O'Donnell, D., Paynter, D. J., Persad, G. G., Rumbold, S. T., Takemura, T., Tsigaridis, K., Undorf, S., and Westervelt, D. M.: The Regional Aerosol Model Intercomparison Project (RAMIP), Geosci. Model Dev. Discuss., 2022, 1-40, https://doi.org/10.5194/gmd-2022-249, 2022.

World Health Organization: WHO global air quality guidelines: particulate matter ($PM_{2.5}$ and PM_{10}), ozone, nitrogen dioxide, sulfur dioxide and carbon monoxide, World Health Organization, https://apps.who.int/iris/handle/10665/345329, 2021.

Wu, J., Shi, Y., and Xu, Y.: Evaluation and Projection of Surface Wind Speed Over China Based on CMIP6 GCMs, J. Geophys. Res. Atmos., 125, e2020JD033611, https://doi.org/10.1029/2020JD033611, 2020.

Wu, T., Lu, Y., Fang, Y., Xin, X., Li, L., Li, W., Jie, W., Zhang, J., Liu, Y., Zhang, L., Zhang, F., Zhang, Y., Wu, F., Li, J., Chu, M., Wang, Z., Shi, X., Liu, X., Wei, M., Huang, A., Zhang, Y., and Liu, X.: The Beijing Climate Center Climate System Model (BCC-CSM): the main progress from CMIP5 to CMIP6, Geosci. Model Dev., 12, 1573-1600, https://doi.org/10.5194/gmd-12-1573-2019, 2019.

Xu, Y., Wu, J., and Han, Z.: Evaluation and Projection of Surface $PM_{2.5}$ and Its Exposure on Population in Asia Based on the CMIP6 GCMs, Int. J. Environ. Res. Public Health, 19, 12092, https://doi.org/10.3390/ijerph191912092, 2022.

Yang, X., Zhou, B., Xu, Y., and Han, Z.: CMIP6 Evaluation and Projection of Temperature and Precipitation over China, Adv. Atmos. Sci., 38, 817-830, https://doi.org/10.1007/s00376-021-0351-4, 2021.

Zhai, S., Jacob, D. J., Wang, X., Shen, L., Li, K., Zhang, Y., Gui, K., Zhao, T., and Liao, H.: Fine particulate matter ($PM_{2.5}$) trends in China, 2013–2018: separating contributions from anthropogenic emissions and meteorology, Atmos. Chem. Phys., 19, 11031-11041, https://doi.org/10.5194/acp-19-11031-2019, 2019.

Zhai, S., Jacob, D. J., Wang, X., Liu, Z., Wen, T., Shah, V., Li, K., Moch, J. M., Bates, K. H., Song, S., Shen, L., Zhang, Y., Luo, G., Yu, F., Sun, Y., Wang, L., Qi, M., Tao, J., Gui, K., Xu, H., Zhang, Q., Zhao, T., Wang, Y., Lee, H. C., Choi, H., and Liao, H.: Control of particulate nitrate air pollution in China, Nat. Geosci., 14, 389-395, https://doi.org/10.1038/s41561-021-00726-z, 2021.

https://doi.org/10.5194/egusphere-2023-2370
Preprint. Discussion started: 16 November 2023

Zhang, L., Li, J., Jiang, Z., Dong, Y., Ying, T., and Zhang, Z.: Clear-Sky Direct Aerosol Radiative Forcing Uncertainty Associated with Aerosol Optical Properties Based on CMIP6 Models, J. Climate, 35, 3007-3019, https://doi.org/10.1175/JCLI-D-21-0479.1, 2022.

Zhang, Q., Jiang, X., Tong, D., Davis, S. J., Zhao, H., Geng, G., Feng, T., Zheng, B., Lu, Z., Streets, D. G., Ni, R., Brauer, M., van Donkelaar, A., Martin, R. V., Huo, H., Liu, Z., Pan, D., Kan, H., Yan, Y., Lin, J., He, K., and Guan, D.: Transboundary health impacts of transported global air pollution and international trade, Nature, 543, 705-709, https://doi.org/10.1038/nature21712, 2017.

Zhao, A., Ryder, C. L., and Wilcox, L. J.: How well do the CMIP6 models simulate dust aerosols?, Atmos. Chem. Phys., 22, 2095-2119, https://doi.org/10.5194/acp-22-2095-2022, 2022.

Zheng, B., Tong, D., Li, M., Liu, F., Hong, C., Geng, G., Li, H., Li, X., Peng, L., Qi, J., Yan, L., Zhang, Y., Zhao, H., Zheng, Y., He, K., and Zhang, Q.: Trends in China's anthropogenic emissions since 2010 as the consequence of clean air actions, Atmos. Chem. Phys., 18, 14095-14111, 10.5194/acp-18-14095-2018, 2018.

Zhu, H., Jiang, Z., Li, J., Li, W., Sun, C., and Li, L.: Does CMIP6 Inspire More Confidence in Simulating Climate Extremes over China?, Adv. Atmos. Sci., 37, 1119-1132, https://doi.org/10.1007/s00376-020-9289-1, 2020.

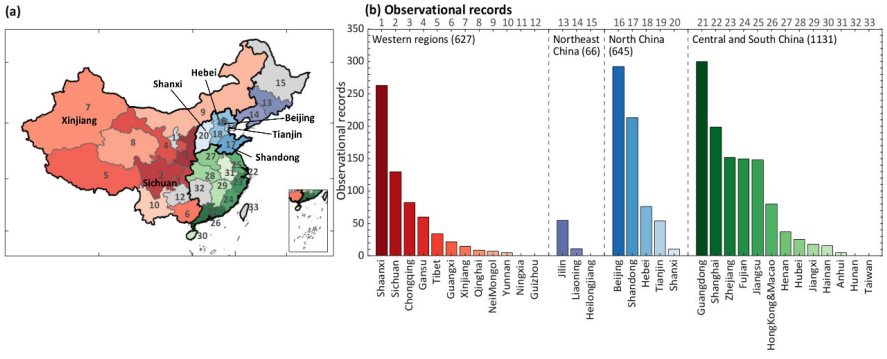

Figure 1. Observational records of $PM_{2.5}$ components during 2000–2014 collected from the literature. (a) The map depicts individual provinces in four regions, including the western regions in red colors, Northeast China in purple, North China in blue, and Central and South China in green. The provinces without observational records are in gray. The number denotes each province. (b) Provincial observation records in China. The number in the upper x-axis and the color in each bar match the province in (a).

https://doi.org/10.5194/egusphere-2023-2370
Preprint. Discussion started: 16 November 2023

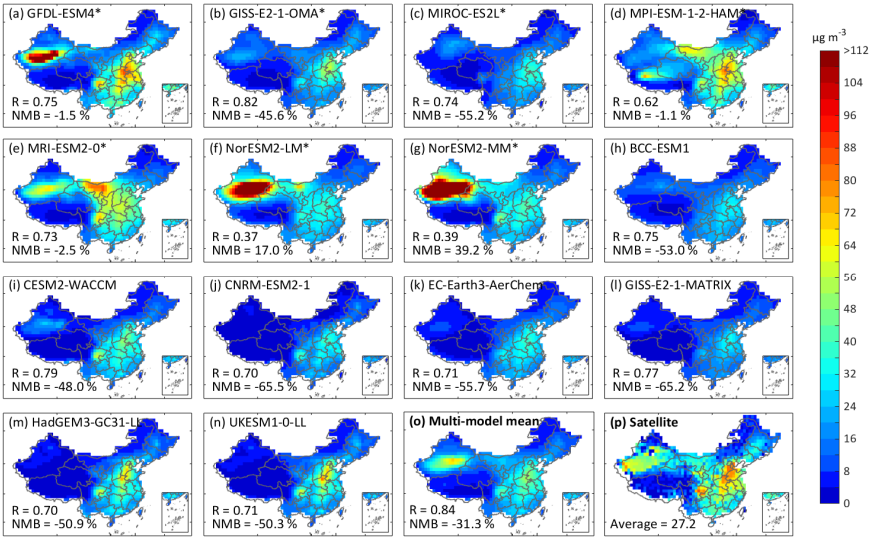

Figure 2. Multi-year mean annual average near-surface total $PM_{2.5}$ concentrations over China during 2000–2014. (a-g) Model outputted $PM_{2.5}$ concentrations in seven models. (h-n) Calculated $PM_{2.5}$ concentrations in the other seven models according to Eq. 1. (o) Multi-model mean. (p) Satellite-based total $PM_{2.5}$ dataset.

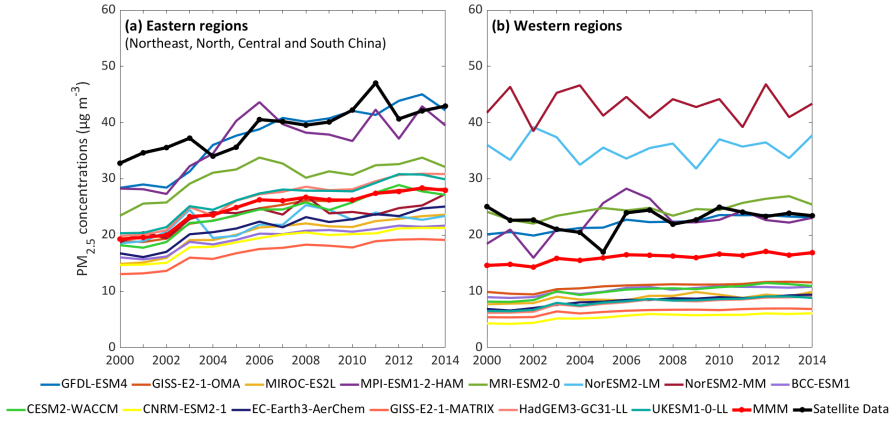

Figure 3. Time series of annual mean regional average total $PM_{2.5}$ concentrations. (a) Over the eastern regions (including Northeast China, North China, and Central and South China). (b) Over the western regions. The bold black lines denote satellite-based $PM_{2.5}$ concentrations, and the bold red lines denote multi-model mean (MMM) concentrations.

https://doi.org/10.5194/egusphere-2023-2370
Preprint. Discussion started: 16 November 2023

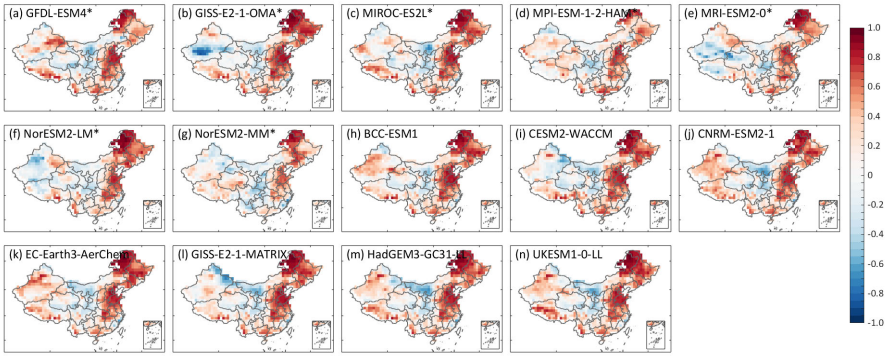

Figure 4. Spatial distribution of correlation coefficients between modeled and satellite-based data for interannual variations of annual mean total $PM_{2.5}$ concentrations over 2000–2014.

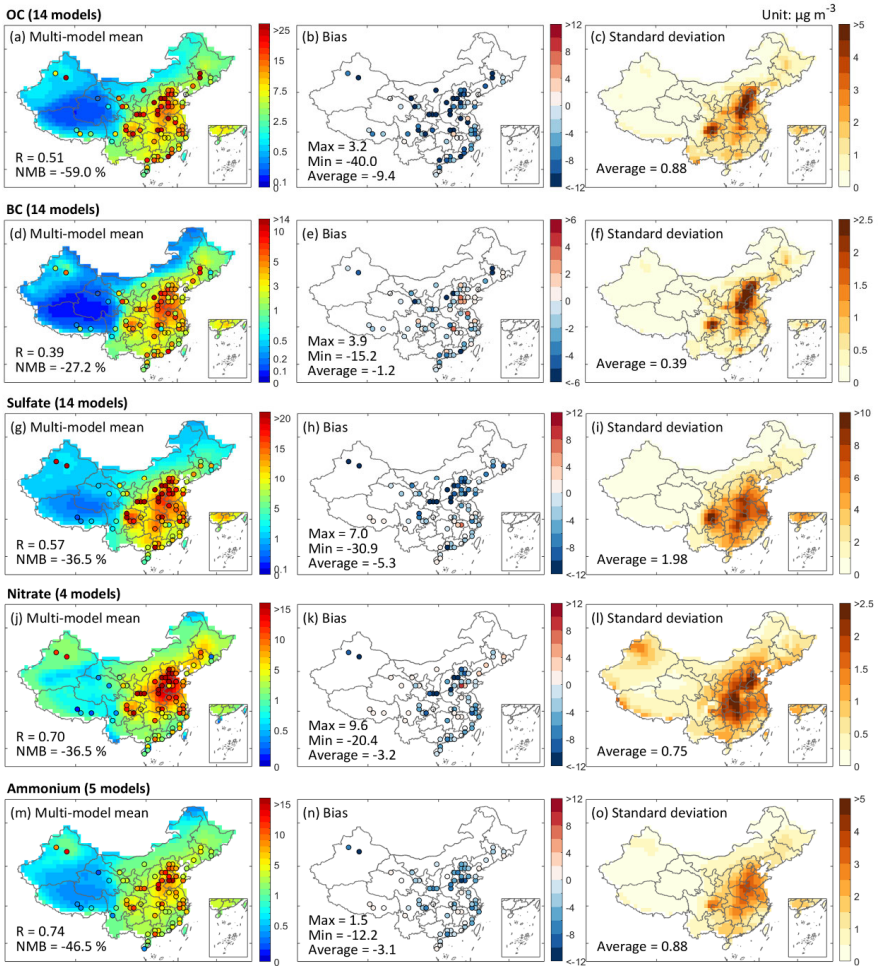

https://doi.org/10.5194/egusphere-2023-2370
Preprint. Discussion started: 16 November 2023

669 **Figure 5. The spatial distribution of multi-year averages of modeled $PM_{2.5}$ components during 2000–2014.**
670 **(First column) The multi-model mean $PM_{2.5}$ component concentrations, overlaid with average ground-based**
671 **observations in filled circles. (Second column) The bias of multi-model mean concentrations. (Third column)**
672 **The standard deviation of $PM_{2.5}$ component simulations among the CMIP6 models.**

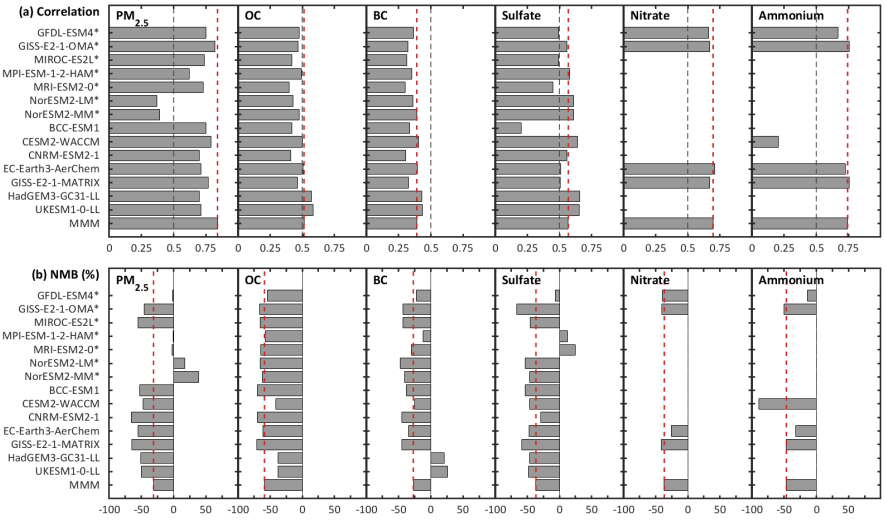

673

674 **Figure 6. Multi-year mean spatial correlation and bias for $PM_{2.5}$ components over 2000–2014 for individual**
675 **models. Results for total $PM_{2.5}$ refer to the comparison against the satellite-based dataset, and those for**
676 **components are relative to the observations compiled from the literature. The red dotted lines denote multi-**
677 **model mean (MMM).**

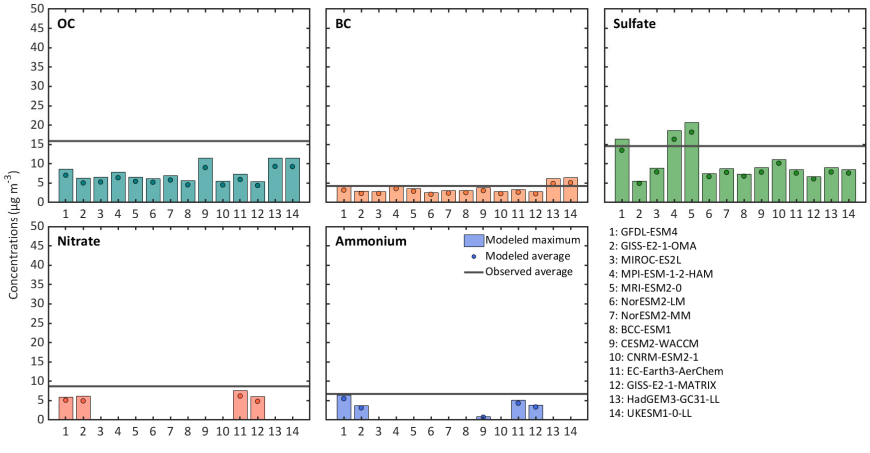

678

679 **Figure 7. Maximum and average concentrations over 2000–2014 for simulated national mean $PM_{2.5}$**

https://doi.org/10.5194/egusphere-2023-2370
Preprint. Discussion started: 16 November 2023

components simulated by individual models. In each year, model values are sampled from grid cells with available observations.